FISHERIES OCEANOGRAPHY

Testing a model to track marine fish migrations in polar regions using pop-up satellite archival tags

Journal:	*Fisheries Oceanography*
Manuscript ID:	FOG-11-0941.R1
Manuscript Type:	Original Article
Date Submitted by the Author:	n/a
Complete List of Authors:	Chittenden, Cedar; University of Tromso, Arctic and Marine Biology ÃÂ dlandsvik, Bjorn; Institute of Marine Research, Norway, Oceanography & Climate Pedersen, Ole-Petter Righton, David Rikardsen, Audun
Keywords:	Barents Sea < region, salmon < fish < taxon, migration < biological processes, management < fishery, temperature < remote sensing < method, tagging < method, analytical < model

Testing a model to track fish migrations in polar regions using pop-up satellite archival tags

CEDAR M. CHITTENDEN[1], *BJØRN ÅDLANDSVIK[2], OLE-PETTER PEDERSEN[1], DAVID RIGHTON[3] AND AUDUN H. RIKARDSEN[1,4]

[1]*Department of Arctic and Marine Biology, University of Tromsø, N-9037 Tromsø, Norway*

[2]*Institute of Marine Research, P.O. Box 1870, Nordnes, N-5817 Bergen, Norway*

[3]*Center for Environment, Fisheries and Aquaculture Science, Pakefield Road, NR33 0HT Lowestoft, UK*

[4]*Norwegian Institute for Nature Research (NINA), FRAM-Centre, N-9296 Tromsø, Norway*

**Correspondence*. e-mail: bjorn@imr.no

ABSTRACT

The use of pop-up archival satellite tags (PSATs) to geolocate marine fishes in polar regions is challenging due to the brevity of periods during which there is a defined sunrise and sunset. Models using other environmental parameters are thus required to supplement geolocation data in the estimation of marine migratory routes. For this study, a state-space model that could create biased random walks using temperature and depth recordings was adapted to track migrating Atlantic salmon (*Salmo salar*). Estimated geolocations from PSATs were used to test and constrict the model. The model's predicted migratory routes were within 100 km of the light-based geolocations calculated by the tags. By constraining the trajectories through the geolocations, bias was reduced. Sensitivity analyses demonstrated that slight alterations of the location and timing of the start and end points did not affect the mean migratory route estimates. This method is a management tool that can determine the primary habitat areas for any surface- or bottom-dwelling marine species—especially in polar regions, where other methods may be impossible.

Key words: Arctic, Atlantic Ocean, Barents Sea, migration, open ocean, SST, telemetry

INTRODUCTION

Satellite telemetry has been used for decades to track marine migratory species, including reptiles (e.g. Luschi *et al*., 1996; Hughes *et al*., 1998), birds (e.g. Jouventin and Weimerskirch, 1990; Georges *et al*., 1997), and mammals (e.g. Lowry *et al*., 1998; Richards *et al*., 1998). As satellite tags do not require an animal to be recaptured in order for data to be obtained, they are particularly useful for species with long migrations in the open ocean (Mate *et al*., 1998; Gillespie, 2001). However, for data to be uploaded to a satellite, the tag's antenna must be pointing upward and in air—making the study of most teleost fish species all but impossible. Pop-up satellite archival tags, or PSATs, are an advanced technology created for the study of such species (e.g. Lutcavage *et al*., 1999). PSATs are buoyant and can be programmed to release from a tagged animal on a certain date, or when an animal has remained at a constant depth for a pre-determined period of time (in the case of a probable mortality). Once at the surface, the tag transmits as much stored environmental data as possible to passing satellites. The first PSATs could only be used on large marine fish species (e.g. Lutcavage *et al*., 1999; Arrizabalaga *et al*., 2008), but recent size reductions have enabled their use with smaller species (e.g. Aarestrup *et al*., 2009).

PSATs generally record temperature, depth and light intensity at regular time intervals, although other types of environmental sensors can be attached (e.g. salinity, chlorophyll recorders; Teo *et al.,* 2009). Algorithms programmed into the tags calculate geolocations (latitude and longitude) using estimates of sunrise and sunset derived from collected light-level data. For locations at which sunset and sunrise are defined by rapid and large changes in the visible light-level, light-based geolocation is generally effective. However, at polar latitudes (north of the Arctic Circle and south of the Antarctic Circle), accurate geolocation estimates are possible only during brief periods before and after the spring and autumn equinoxes (Fig. 1). During these times, estimating geolocation is possible, but still challenging for a few reasons. The duration of twilight is greater at higher than at lower latitudes, making estimations of exact sunrise and sunset times difficult, especially with any additional factors affecting light levels (e.g. diving behaviours or adverse weather conditions). Furthermore, the difference in irradiance between day and night is reduced in polar regions (Fig. 1), adding more error to estimates.

Most PSAT-based studies of the migratory behaviour of marine animals have been focused on species residing at more temperate latitudes, such as bluefin tuna (Block *et al*., 2005) or leatherback turtles (Hays *et al*., 2006). Information on the migration and distribution of fishes at high latitudes is also of great importance though, as these areas support some of the largest commercial fisheries in the world and many of these stocks are becoming severely depleted (Sakshaug *et al.* 2009). For example, anadromous Atlantic salmon (*Salmo salar*) and Pacific salmon species (*Oncorhynchus* spp.) undertake long foraging migrations into northern oceans where observational studies are challenging (Hansen *et al*., 1993; Hansen and Quinn, 1998; Rikardsen *et al*., 2008; Thorstad *et al.*, 2011). The open-ocean migratory behaviour of salmonids has been pieced together over the last century from fishery-catch data and mark-recapture studies (Hansen *et al.,* 1993; Hansen and Jacobsen, 2000; Rikardsen *et al.*, 2008). However, there exists almost no data beyond commonly fished areas, and without any continuous real-time data, great knowledge gaps and bias exist in terms of the marine distribution of salmonids (Devineau *et al.* 2006; Chittenden *et al.*, 2009). PSATs may help researchers to overcome these problems; however, at polar latitudes, other geolocation methods are required.

A number of approaches have been applied to the problem of estimating the migratory pathways of animal species. In general, they differ with respect to the applied theoretical frameworks, forcing fields, and data assimilation methods (i.e. to which extent the model is able to incorporate and use external data as correctors). In the simplest cases, models were developed to reconstruct the horizontal movements of migrating fish by matching hydrographical fields with data collected by tagged fish (Metcalfe and Arnold, 1997; Righton and Mills, 2006; Tremblay *et al.*, 2009). More complex models use various statistical techniques, including Bayesian models (Kurota *et al.*, 2009), bootstrapping techniques (Tremblay *et al.*, 2009), and weighted kernel estimation techniques (Walli *et al.*, 2009) to provide estimates of location. The number of modeled and measured physical fields that have been applied to force and correct migratory trajectories is continually increasing (Booker *et al.*, 2008; Patterson *et al.*, 2008; Schick *et al.,* 2008).

State-space models (SSMs) are emerging as the leading method to estimate animal movement behaviour due to their statistical robustness and predictive ability (Patterson *et al.*, 2008). Typical SSMs require data input in the form of many location points from a few individuals, or a few location points from many individuals (Patterson *et al.*, 2008). In polar regions, however, these types of data may not be possible to obtain. In addition to the previously mentioned challenges associated with geolocating at high latitudes, the fishing effort in the open ocean is practically non-existent for many species, including Atlantic salmon. Thus, to be able to estimate the marine movement behaviour of Atlantic salmon in polar regions, a simple model adapted to the scarce location data is required. The ideal model would create possible tracks for each individual using only sea-surface temperature (SST) and depth, and could be tested and improved with available geolocation data points.

Ådlandsvik *et al.* (2007) created a simple model that incorporated a forward/backward-Lagrangian model with a biased random walk to re-construct the migratory pathways of individual Northeast Arctic cod (*Gadus morhua* L.) using only temperature and depth. This model could not be used directly on Atlantic salmon data however, for cod are bottom-dwellers and Atlantic salmon are surface-oriented during their marine phase (Rikardsen and Dempson, 2011). To be able to use the model with Atlantic salmon, it first needed to be adapted to reflect the behaviour of a surface-dwelling species.

The objectives of this work were to

- adapt the method of Ådlandsvik *et al*., (2007) to fit a surface-dwelling species,
- test the results with validated PSAT geolocation data,
- run a sensitivity analysis on the model to see if altering the start and end times and locations affect the results, and
- use validated geolocations as waypoints to constrain the model and improve the accuracy of the predicted trajectories.

MATERIALS AND METHODS

The salmon data

Two PSAT datasets from female Atlantic salmon kelts were used to test the model (Fish 1: 111 cm long, 9.9 kg; Fish 2: 101 cm long, 7.6 kg). A ‘kelt’ is a post-spawned adult salmon that leaves its freshwater spawning grounds to return to ocean feeding areas (Halttunen *et al.*, 2009). The fish were caught by angling during May 2008 in the Alta River (70°N 23°E), which enters the Altafjord, in northern Norway (Fig. 2). They were transported to a marine pen (5x5x5 m) approximately 5 km away from the Alta River estuary. The fish were kept in the marine pen for one week, to acclimatise to the salt water prior to their tagging and release. The fish were anaesthetized for surgery (2-phenoxy-etanol, 0.5 mL L^{-1}, mean time 3 min) and placed in a water-filled tube with their head and gills submerged. A PSAT tag, recording temperature, depth and light-based geolocation (Model: X-tags; 12 cm length + 20 cm antenna, diameter 16 - 32 mm, mass 42 g in air, Microwave Telemetry Inc., Colombia, MD, USA), was attached externally to each fish by bridling the tag to two cushioned bio-compatible backplates that were wired through the dorsal musculature below the dorsal fin. A small acoustic transmitter (9 mm diameter, Thelma Biotel, Norway) was also attached to one of the backplates, and the fjord entrance was monitored with an array of hydrophones (Vemco VR2, Nova Scotia, Canada, see Halttunen *et al.*, 2009) so that the exact date that the fish left the fjord could be determined for the start date of the model. The tagged fish were released immediately into the Altafjord following surgery on 22 May 2008, after which they took approximately three days to exit at location “B” (Fig. 2).

Tag effect studies of PSATs on Atlantic salmon have not yet been published. However, recaptures of salmon after one year at sea with the tags/harnesses still attached have demonstrated that the attachment technique works well and the fish are able to complete their marine phase and return to fresh water (Rikardsen *et al.,* unpublished data). The two tags released from their attachments due to their being at a constant depth for four consecutive days (Tag 1 after 181 days on 19 November 2008 and a minimum distance travelled of 472 km, and Tag 2 after 146 days on 15 October 2008 and a minimum distance travelled of 579 km). It is likely that the tags and harnesses had detached from the fish, either due to shedding or predation, and drifted with surface currents for four days prior to uploading their location and archived data to the ARGOS satellites. Therefore, a back-calculation of the initial pop-up location was required. The real-time ARGOS geolocation on the fourth day after the tag initiated contact with the satellites was used to determine the four-day change in latitude and longitude experienced by the tags due to surface currents. These latitudinal and longitudinal differences were then subtracted from the initial pop-up location to give the estimated pop-up site (a correction of 0.248ºS, 3.183ºE for Tag 1, and 0.196ºS, 1.403ºW for Tag 2).

A total of 78% of the data for Tag 1 and 87% of the data for Tag 2 were downloaded by the ARGOS satellites. The tag data were prepared for the model by computing the maximum hourly depth and the hourly mean temperature recorded at a swimming depth of 0 m. Any missing data were filled in by linear interpolation. Rapid changes in temperature recorded by the tag were smoothed by a 7-day moving average, to fit the lower (weekly) resolution of the SST archive used in the model.

As geolocation estimates from tags deployed in polar regions are unreliable during most of the year, the data required filtering before it could be used. Previous work validated geolocation estimates against SST data (Teo *et al.*, 2004; Nielsen *et al.*, 2006; Pedersen *et al.,* 2011). Here, a first filtering removed the geolocations that were on land and those occurring from 10 d before the autumnal equinox (22 September 2008) to 10 d after (at the equinox, daylength is nearly the same at all latitudes so latitude estimates become inaccurate). A second filtering removed those data points that had temperatures 0.25°C above or below the actual sea-surface temperature (SST) at that location. Four temperature parameters were calculated from the tag data to estimate the SST at each location: 1) the mean daily temperature recorded from 0-5 m, 2) the mean daily temperature recorded at 0 m only, 3) the maximum daily temperature at 0 m, and 4) the minimum daily temperature at 0 m. If at least three out of four of the tag SST estimates was within ± 0.25°C of the actual SST data (within 0.5° latitude and longitude of each geolocation provided by the tags), the geolocation passed the second filtering. Daily SST data with "an RMS error of less than 0.6 K at high resolution" (Stark *et al.,* 2007) were provided by OSTIA (http://ghrsst-pp.metoffice.com/pages/latest_analysis/ostia.html). A third filtering removed any geolocation that required a swimming speed of >2 m/s to reach from the previous location, which would be unrealistic for an adult Atlantic salmon (Halttunen *et al.,* 2009; Thorstad *et al*., 2011). The remaining geolocations were then split into two groups—those recorded before the equinox (one location for Tag 1, nine locations for Tag 2), and those recorded afterwards (three locations for Tag 1, two locations for Tag 2), and averaged. This was done to give a more general migratory pathway and smooth the individual geolocation estimates, as they have been found to have errors of up to 100 km (Musyl *et al.* 2001).

Adapting the model

The model in Ådlandsvik *et al.* (2007) creates trajectories consistent with the available information from each tag. Two sets of trajectories are generated—one progressing forward in time from the start site, and one progressing backward from the final (corrected pop-up or geolocation) position. The trajectories progress by combining a deterministic and a stochastic velocity component. The deterministic component pulls the particle forward at a velocity that would get the particle to the final position during the time available. The stochastic component is a random walk velocity, with a fixed speed and an arbitrary/random direction.

After each internal time step (one hour), the environmental dataset (depth and temperature) was sampled at the position of the trajectory. If the tag data were not consistent with the environmental data at the new position, the trajectory was given a second chance by returning it to the previous position. If the previous position was also inconsistent with the environmental data at the new time (for instance due to a deep dive), the trajectory was terminated. As a final step, the forward and backward trajectories were merged at the temporal midpoint between the release and pop-up sites. This was done by looping through the active forward trajectories and choosing the nearest backwards trajectory if the midpoint positions were closer than a given threshold (for further details and a step-by-step guide to the trajectory algorithm, see Ådlandsvik *et al.,* 2007).

To adapt the model used in Ådlandsvik *et al.* (2007) to the surface-oriented Atlantic salmon data, sea-surface temperature (SST) was used instead of temperature estimates from the entire water column. The SST data were acquired from the gridded dataset

NOAA_OI_SST_V2, which is provided online by the NOAA Earth System Laboratory on their website http://www.esrl.noaa.gov/psd/ (Reynolds *et al.,* 2002). This dataset has one degree of spatial and one week of temporal resolution.

Sub-grid variation in the environmental data was accounted for in the model with termination thresholds (Table 1). These parameters had to be narrow to ensure that the termination criteria were effective and provided adequate selection pressure for the trajectories. However, they also needed to be flexible enough to give a reasonable ensemble of active trajectories. The values were determined by trial and error. Additional sensitivity analyses (not presented here) found that the results were not sensitive to the precise value of these parameters, as long as they demonstrated a reasonable number of tracks and adequate selection pressure. For Tag 1, the start location was moved outside the fjord, requiring a later start date than the actual deployment. For Tag 2 the start location was kept inside the Altafjord, requiring the depth factor to be increased to 1.3, and the temperature threshold dT to be increased to 1.5°C to allow the particles to survive the narrow constraints within the fjord.

The model samples the datasets at the track positions by multi-linear interpolation. For temperature (T), a symmetric two-sided criterion was used. Each trajectory had to satisfy the criterion:

$$| T_{SST} - T_{tag} | < dT \qquad \text{(Equation 1)}$$

where T_{tag} is the temperature recorded by the tag, T_{SST} is the interpolated temperature from the database and dT is the temperature threshold.

For depth, the gridded ETOPO1 bathymetry dataset was obtained from the NOAA National Geophysical Data Center (http://www.ngdc.noaa.gov/mggd/; Amante and Eakins, 2009). This data set has a resolution of one minute latitude/longitude. Depth was used as a one-sided limiter terminating trajectories where the sampled depth H_{etopo} was shallower than the tag's recorded depth H_{tag}. The limiter had the following algebraic formulation:

$$H_{tag} < a*H_{etopo} + H_0 \qquad \text{(Equation 2)}$$

where a is a coefficient and H_0 is an additive depth offset.

A sensitivity analysis was conducted to determine whether the model output would vary if the start location, start date, end location, or end date were altered slightly (Table 2). For this analysis, a standard run of the model (A) was conducted with certain parameters changed (A2, A3, B, C, D, Table 2).

RESULTS

Modeling Atlantic salmon tracks

For Tag 1, a total of 21,556 merged tracks resulted from 100,000 initial trajectories (Fig. 3a). The mean track headed northwards for the first 60 days, then turned southwards for 40 days before heading northwards again, and veering northeast along the 400 m isobaths (Fig. 3a). When the tag data (Fig. 3b) were compared with the modelled tracks, we found that the kelts undertook some deep dives at the end of July (>300 m), which meant that the trajectory had to go straight north to reach the deeper areas by that time. Towards the end of August and during the first half of September, the temperature recordings increased (>9°C), which meant that the fish must have been further south to fit the SST data. From the end of September onward, the kelts began diving more deeply again (>400 m), which forced the non-terminated tracks northward to the Bear Island Trench. The colder temperature recordings and the short period before the pop-up date then forced the tracks towards the northeast.

For Tag 2, a total of 121 merged tracks resulted from 100,000 initial trajectories (Fig. 3c). The data from Tag 2 also showed deep dives during late July (~300 m, Fig 3d). However, as the dives were slightly shallower than those for Tag 1, the trajectories were not forced so far northward as they were for Tag 1 (Fig. 3). Without any further depth constraints the track for Tag 2 veered further east and progressed at a steady pace towards the pop-up location (Fig. 3c). The more easterly track distribution is consistent with the colder temperatures recorded by Tag 2 (Figs. 3b, d).

Testing the model with geolocations

As the study took place north of 70ºN, reliable geolocations were possible to obtain from irradiance during two brief periods—late August to early September, and October (Fig. 1). Tag 1 had a greater number of rejected geolocation estimates, and fewer validated geolocation estimates than Tag 2 (Fig. 4). When the model was tested against the valid geolocations for Tag 1, three out of the four geolocations overlapped the model's centre of gravity (the mean location of the particle locations ± standard deviation, on the day of the geolocation estimate; Fig. 5a). For Tag 2, most of the 12 geolocations were further east than, but within 100 km of the centre of gravity of the modelled particles (Fig. 5b).

Model sensitivity analysis

A sensitivity analysis run on the model using the data from Tag 1 found that the mean of the trajectories did not change greatly (<50 km) when the start or end date were altered by <3 d (Fig. 6). Moving the start and end locations <100 km also did not change the overall pattern formed by the data from the tag and the environment (Fig. 6a). After 40 d, the mean trajectories were primarily within 40 km of the standard run A (Fig. 6b).

Constraining the model through geolocations

When the model was run using the validated geolocations as waypoints, the number of trajectories was reduced and the routing of the means was altered (Fig. 7). The mean trajectory of Tag 1 did not change greatly when constrained through the geolocations. However, as the geolocations estimated by Tag 2 were situated beyond the pop-up location, its trajectories were pulled eastward.

DISCUSSION

During times when it is not possible to monitor migrating marine fishes using light-based geolocation, other methods are required. The simple model from this study was successful at estimating likely migratory routes of Atlantic salmon using only the temperature and depth recordings from a PSAT tag. Sensitivity analyses found that slight alterations of the start and end points in space and time did not change the overall mean trajectory routes, suggesting that the reconstructed tracks reflect the actual migration of the individual fish, rather than model artifacts. In particular, errors induced by moving the start position out of the fjord, and by back-calculating the release position, did not influence the overall results. The accuracy of the model was easily increased by constraining the trajectories through filtered geolocations; adding further limiting environmental parameters to the model (e.g. salinity) would do the same. This method has potential as a tool to track marine fish species at polar latitudes, where other methods may be too difficult or impossible.

Patterson *et al*. (2008), in their review of tracking models, describe SSMs as time-series models that "predict the future state of a system from its previous states probabilistically, via a process model." Typically the SSMs in this review have many locational data points, and deal with the challenges of data smoothing and understanding the behaviours associated with spatial-temporal patterns in the data. To follow the large-scale movements of Atlantic salmon at sea with only temperature and depth data, and only a few locational points, a different sort of SSM was required for this work. A simple SSM created to track bottom-dwelling Northeast Arctic cod (Ådlandsvik *et al*., 2007) was adapted to fit surface-oriented species, likely increasing its accuracy, as SST estimates are more reliable than temperatures estimated at depth due to higher spatial and temporal resolution.

The approach taken for this study was similar to the particle filter approach taken for cod by Anderson *et al*. (2007). Both methods obtain ensembles of trajectories consistent with the available data. However, the method used by Anderson *et al*. produces estimates of the probability of the trajectories by carrying out a probability-weighted resampling of the trajectories at every time step while the current method simply terminates trajectories considered impossible. Both methods have a subjective element in assigning probability distributions to termination criteria. For a bottom-dwelling fish like cod, the tag data provides estimates of the bottom depth. For Atlantic salmon, only minimum depth estimates may be obtained. A probability distribution in this case would be more or less flat for the water column and not too different from our termination criteria. The problem is symmetric with respect to time reversal; due to the forward and backward trajectories and the merge step, the approach of Ådlandsvik *et al.* (2007) respects this time symmetry. The particle filter approach could easily be made time symmetric using a similar procedure.

It has been hypothesised that migratory fishes use oceanic currents to reach marine feeding grounds (Dadswell *et al.,* 2010). As the probable trajectories estimated by the model went northward with the offshore currents, they were consistent with this hypothesis as well as with previous mark-recapture studies (Hansen *et al.*, 1993; Rikardsen *et al.*, 2008; Rikardsen and Dempson, 2011; Thorstad *et al*., 2011). A novel discovery, however, was that both the trajectories and validated geolocations of Tag 2 indicated that it had travelled further east into the Barents Sea than had been reported by any previous Atlantic salmon tagging study (Rikardsen *et al.,* 2008; Thorstad *et al*., 2011).

The modelled trajectories were initially terminated due to reasons of depth—i.e. the depth recording from the tag was greater than the depth at the modelled particle's location. The data showed that the salmon left the coastline area fairly quickly—likely within one month post-release. Further along the migratory route, in the Barents Sea, temperature became the more limiting factor. The Barents Sea has a large SST gradient as a result of warmer Atlantic waters from the southwest mixing with cooler Arctic waters from the northeast (the polar front; Sakshaug *et al.*, 2009). This high degree of temperature variation allowed for more precision in modelling the migratory routes of salmon when depth was fairly uniform.

In addition to temperature and depth, other environmental parameters, such as salinity, chlorophyll, and magnetic field, could be used to constrict the model. Longitude estimates could also improve the accuracy of the trajectories. PSAT tags are able to calculate longitude more frequently and more accurately than latitude (Hill and Braun, 2001). This discrepancy is especially prominent in polar regions.

All geolocations used in accuracy testing first had to pass a rigorous validation method, as the geolocations themselves have some error (Musyl *et al.*, 2001). A greater number of geolocations were deemed valid for Tag 2, which may have been a result of clearer weather in the eastern Barents Sea where the tag was located, allowing for a more precise measurement of sunrise/sunset time. The model results were consistent with the PSAT-estimated geolocations, but demonstrated some bias when the geolocations were located beyond the pop-up location (i.e. when the pop-up location was closer to the release site than the estimated geolocations). In such cases, the model's deterministic velocity component pulled particles on a more direct routing toward the pop-up location. When the trajectories were constrained to pass through the smoothed pre- and post-equinox geolocation points, however, this bias was removed.

CONCLUSION

This simple model is a straightforward way to reliably predict the migratory routes of bottom- and surface-dwelling marine species using archival tag data (in this case, temperature and depth). The method's strength is its ability to track fish in polar regions, where geolocation estimates are not possible during most of the year. Sensitivity analyses found little effect on the results from spatial and temporal alterations of the start and end points, and accuracy testing found the results were consistent with validated tag geolocations. For added accuracy, the model can be constrained through geolocation estimates from PSAT tags, or by other types of archival data such as salinity, chlorophyll, or magnetic field. Technological advances in PSAT telemetry that offer multiple, sequential pop-off options (Microwave Telemetry, Inc., MD, USA) could enable further accuracy checks of the model and provide greater locational data availability for fish in polar regions.

ACKNOWLEDGEMENTS

We thank Kathrine Michalsen, Finn Økland, Tor Næsje, Jenny Jensen, Jan Davidsen, Elina Halttunen, Ceselie Lien, and Amund Suhr for their assistance, and the Tromsø Forskningsstiftelse and Alta Laksefiskeri Interessentskap for their financial support.

REFERENCES

Aarestrup, K., Økland, F., Hansen, M.M., Righton, D., Gargan, P., Castonguay, M., Bernatchez, L., Howey, P., Sparholt, H., Pedersen, M.I., and McKinley, R.S. (2009) Oceanic Spawning Migration of the European Eel (*Anguilla anguilla*). *Science* **325**: 1660.

Amante, C. and Eakins, B.W. (2009) ETOPO1 1 Arc-Minute Global Relief Model: Procedures, Data Sources and Analysis. NOAA Technical Memorandum NESDIS NGDC-24, March 2009, 19 pp.

Andersen, K.H., Nielsen, A., Thygesen, U.H., Hinrichsen, H.-H., and Neuenfeldt, S. (2007) Using the particle filter to geolocate Atlantic cod (*Gadus morhua*) in the Baltic Sea, with special emphasis on determining uncertainty. *Can. J. Fish. Aquat. Sci.* **64:**(4) 618-627.

Arrizabalaga, H., Pereira, J.G., Royer, F., Galuardi, B., Goni, N., Artetxe, I., Arregi, I., and Lutcavage, M. (2008) Bigeye tuna (*Thunnus obesus*) vertical movements in the Azores Islands determined with pop-up satellite archival tags. *Fish. Oceanog.* **17**: 74–83.

Block, B.A., Teo, S.L.H., Walli, A., Boustany, A., Stokesbury, M.J.W., Farwell, C.J., Weng, K.C., Dewar, H., and Williams, T.D. (2005) Electronic tagging and population structure of Atlantic bluefin tuna. *Nature* **434**: 1121–1127.

Booker, D.J., Wells, N.C., and Smith, P.I. (2008) Modelling the trajectories of migrating Atlantic salmon (*Salmo salar*). *Can. J. Fish. Aquat. Sci.* **65**: 352–361.

Chittenden, C., Beamish, R.J and McKinley, R.S. (2009) A critical review of Pacific salmon marine research relating to climate. *ICES J. Mar. Res.* **66**: 2195–2204.

Dadswell, M.J., Spares, A.D., Reader, J.M., and Stokesbury, M.J.W. (2010) The North Atlantic subpolar gyre and the marine migration of Atlantic salmon *Salmo salar*: the 'Merry-Go-Round' hypothesis. *J. Fish Biol*. **77**: 1095–8649.

Devineau, O., Choquet, R., and Lebreton, J-D. (2006) Planning capture–recapture studies: straightforward precision, bias, and power calculations. *Wildlife Soc. Bull.* **34**(4): 1028–1035.

Georges, J., Guinet, C., Jouventin, P., and Weimerskirch, H. (1997) Satellite tracking of seabirds: interpretation of activity pattern from the frequency of satellite locations. *IBIS*. **139**: 403–405.

Gillespie, T.W. (2001) Remote sensing of animals. *Progr. Phys. Geog*. **25**: 355–362.

Halttunen, E., Rikardsen, A.H., Davidsen, J.G., Thorstad, E.B., and Dempson J.B. (2009) Survival, migration speed and swimming depth of Atlantic salmon kelts during sea entry and fjord migration. In: *Tagging and Tracking of Marine Animals With Electronic Devices, Reviews: Methods and Technologies in Fish Biology and Fisheries 9.* J.L. Nielsen, H. Arrizabalaga, N. Fragoso, A. Hobday, M. Lutcavage, and J. Sibert (eds.) Dordrecht: Springer, pp 35–49.

Hansen, L.P. and Quinn, T.P. (1998) The marine phase of the Atlantic salmon (*Salmo salar*) life cycle, with comparisons to Pacific salmon. *Can. J. Fish. Aquat. Sci.* **55**: 104–118.

Hansen, L.P. and Jacobsen, J.A. (2000) Distribution and migration of Atlantic salmon *Salmo salar* L., in the sea. In: *The Ocean Life of Atlantic Salmon–Environmental* *and Biological Factors Influencing Survival.* D. Mills (ed.) Oxford: Fishing News Books, pp. 75–87.

Hansen, L.P., Jonsson, N., and Jonsson, B. (1993) Oceanic migration in homing Atlantic salmon. *Anim. Behav.***45**: 927–941.

Hays, G.C., Hobson, V.J., Metcalfe, J.D., Righton, D., and Sims, D.W. (2006) Flexible foraging movements of leatherback turtles across the North Atlantic Ocean. *Ecology* **87**: 2647–2656.

Hill, R.D., and Braun, M.J. (2001) Geolocation by light-level. The next step: latitude. In *Electronic tagging and tracking in marine fisheries.* J. Sibert and J. Nielsen (eds.) Kluwer Academic Press, Dordrecht, The Netherlands, pp. 315–330.

Hughes, G.R., Luschi, P., Mencacci, R., and Papi, F. (1998) The 7000-km oceanic journey of a leatherback turtle tracked by satellite. *J. Exp. Mar. Biol. Ecol.* **229:** 209–17.

Jerlov, N.G. and Nielsen, E.S. (1974) *Optical aspects of oceanography*. Academic Press, London, New York, 494 pp.

Jouventin P. and Weimerskirch, H. (1990) Satellite tracking of wandering albatrosses. *Nature* **343**: 746–748.

Kurota, H., McAllister, M.K., Lawson, G.L., Nogueira, J.I., Teo, S.L.H., and Block, B. (2009) A sequential Bayesian methodology to estimate movement and exploitation rates using electronic and conventional tag data: application to Atlantic bluefin tuna (*Thunnus thynnus*). *Can. J. Fish. Aquat. Sci.* **66**: 321–342.

Lowry, L.L., Frost, K.J., Davis, R., DeMaster, D.P., and Suydam, R.S. (1998) Movements and behavior of satellite-tagged spotted seals (*Phoca largha*) in the Bering and Chukchi Seas. *Polar Biol.* **19**: 221–230.

Luschi, P., Papi, F., Liew, H.C., and Chan, E.H. (1996) Long-distance migration and homing after displacement in the green turtle (*Chelonia mydas*): a satellite tracking study. *J. Comp. Physiol.* **178**: 447–52.

Lutcavage, M.E., Brill, R.W., Skomal, G.B., Chase, B.C., and Howey, P.W. (1999) Results of pop-up satellite tagging of spawning size class fish in the Gulf of Maine: do North Atlantic bluefin tuna spawn in the mid-Atlantic? *Can. J. Fish. Aquat. Sci.* **56**: 173–177.

Mate, B.R., Gisiner, R., and Mobley, J. (1998) Local and migratory movements of Hawaiian humpback whales tracked by satellite telemetry. *Can. J. Zool.* **76:** 863–68.

Metcalfe, J.D., and Arnold, G.P. (1997) Tracking fish with electronic tags. *Nature* **387**: 665–666.

Musyl, M., Brill, R., Curran, D., Gunn, J., Hartog, J., Hill, R., Welch, D., Eveson, J., Boggs, C., and Brainard, R. (2001) Ability of archival tags to provide estimates of geographical position based on light intensity. In: *Electronic Tagging and Tracking in Marine Fisheries*. J.R. Sibert and J.L. Nielsen (eds.) Kluwer, Dordrecht, pp. 343–367.

Nielsen, A., Bigelow, K., Musyl, M., and Sibert, J. (2006) Improving light-based geolocation by including sea surface temperature. *Fish. Oceanogr.* **15**: 314–325.

Patterson, T.A., Thomas, L., Wilcox, C., Ovaskainen, O., and Matthiopoulos, J. (2008) State-space models of individual animal movement. *Trends Ecol. Evol.* **23**: 87–94.

Pedersen, M., Patterson, T., Thygesen, U., and Madsen, H. (2011) Estimating animal behavior and residency from movement data. *Oikos.* **120**: 1281–1290.

Reynolds, R.W., Rayner, N.A., Smith, T.M., Stokes, D.C., and Wang, W. (2002) An improved in situ and satellite SST analysis for climate. *J. Climate* **15**: 1609–1625.

Richards, P.R., Heide-Jorgensen, M.P., and Aubin, D.S. (1998) Fall movements of Belugas (*Delphinapterus leucas*) with satellite-linked transmitters in Lancaster Sound, and northern Baffin Bay. *Arctic* **51**: 5–16.

Righton, D. and Mills, C. (2006) Application of GIS to investigate the territorial behaviour of two species of Red Sea butterflyfish. *Int. J. Geogr. Info. Sci.* **20**(2): 215–232.

Rikardsen, A.H., Hansen, L.P., Jensen, A.J., Vollen, T., and Finstad, B. (2008) Do Norwegian Atlantic salmon feed in the northern Barents Sea? Tag recoveries from 70 to 78°N. *J. Fish Biol.* **72**: 1792–1798.

Rikardsen, A.H. and Dempson B. (2011) Dietary life-support: The marine feeding of Atlantic salmon. In: *Salmon Ecology.* Ø. Aas, S. Einum, A. Klemetsen, and J. Skurldal (eds.) Blackwell Publishing Ltd., pp. 115–143.

Sakshaug, E., Johnsen, G., and Kovacs, K. (2009) *Ecosystem Barents Sea.* Tapir Academic Press, Trondheim, 586 pp.

Schick, R., Loarie, S., Colchero, F., Best, B., Boustany, A., Conde, D., Halpin, P., Joppa, L., McClellan, C., and Clark, J. (2008) Understanding movement data and movement processes: current and emerging directions. *Ecol. Letters.* **11**: 1338–1350.

Stark, J.D., Donlon, C.J., Martin, M.J., and McCulloch, M.E. (2007) OSTIA: an operational, high resolution, real time, global sea surface temperature analysis system. Oceans '07 IEEE Aberdeen, conference proceedings. Marine challenges: coastline to deep sea. Aberdeen, Scotland. IEEE.

Teo, S.L., Kudela, R., Rais, A., Perle, C., Costa, D.A., and Block, B.A. (2009) Estimating chlorophyll profiles from electronic tags deployed on pelagic animals. *Aquat. Biol.* **5**: 195–207.

Teo, S.L.H., Boustany, A., Blackwell, S., Walli, A., Weng, K.C., and Block, B.A. (2004) Validation of geolocation estimates based on light level and sea surface temperature from electronic tags. *Mar. Ecol. Prog. Ser.* **283**: 81–98.

Thorstad, E.B, Whoriskey, F., Rikardsen, A.H., and Aarestrup, K. (2011) Aquatic nomads: the life and migrations of the Atlantic salmon. In: *Salmon Ecology*. Ø. Aas, S. Einum, A. Klemetsen, and J. Skurldal (eds.) Blackwell Publishing Ltd., pp. 1–32.

Tremblay, Y., Robinson, P.W., and Costa, D.P. (2009) A parsimonious approach to modelling animal movement data. *PLoS ONE*. **4**:e4711.

Walli, A., Teo, S.L.T., Boustany, A., Farwell, C.J., Williams, T., Dewar, H., Prince, E., and Block, B. (2009) Seasonal movements, aggregations and diving behaviour of Atlantic bluefin tuna (*Thunnus thynnus*) revealed with archival tags. *PLoS ONE*. **4**:e6151.

Ådlandsvik, B., Huse, G., and Michalsen, K. (2007) Introducing a method for extracting horizontal migration patterns from data storage tags. *Hydrobiologia* 582: 187–197.

FIGURES

Figure 1. The theoretical light intensity at sea surface as a function of latitude and time (calculated according to Jerlov and Nielsen, 1974). Whereas geolocation is possible at all times of the year at more temperate latitudes, nearer the poles, geolocation periods (shaded areas) are limited to either side of the equinoxes (E).

Figure 2. The study area in northern Norway. The standard model start location (A) is located near the entrance to the Altafjord. Sensitivity analyses of the model tested various other start locations, indicated as B, C, and D. The black star denotes the release location, where the Alta River enters the Altafjord.

Figure 3. A random selection of 200 possible trajectories for Tag 1 (a) and all 121 trajectories for Tag 2 (c), as well as the archived temperature and depth data from Tag 1 (b) and Tag 2 (d). The red curves in (a) and (c) give the mean of all tracks, and the white disks indicate 10-day intervals.

Figure 4. Map of the geolocations estimated by Tag 1 and Tag 2. Colours denote the reason for the validation or rejection of each geolocation.

Figure 5. Snapshot plots of the centre of gravity (± the standard deviation as an ellipse) for the trajectory particle locations (blue ovals) at the time of each geolocation (red circle) for Tag 1 and Tag 2.

Figure 6. Sensitivity analysis plots of the mean trajectories (a) and distances from the standard run A over time (b) for Tag 1. Parameters for each run are given in Table 2.

Figure 7. Constraining the model through validated geolocations from Tag 1 (a) and Tag 2 (c). Averaging the pre-equinox and post-equinox geolocations for Tag 1 (b) and Tag 2 (d) smoothed the error found in the individual geolocation estimates to show a more general migratory pathway. The release, pop-up and geolocation positions are denoted by stars.

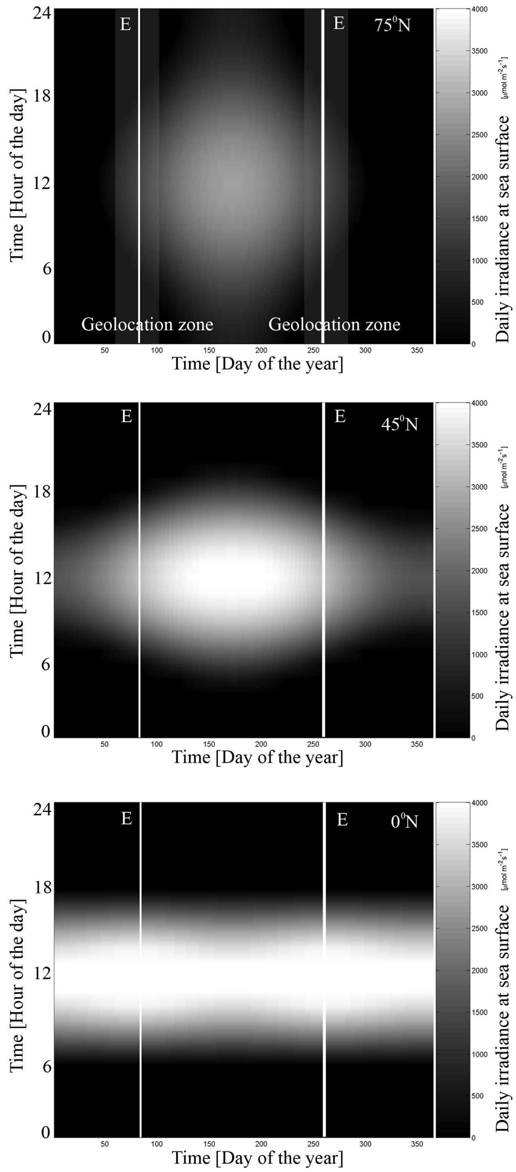

Figure 1. The theoretical light intensity at sea surface as a function of latitude and time (calculated according to Jerlov and Nielsen, 1974). Whereas geolocation is possible at all times of the year at more temperate latitudes, nearer the poles, geolocation periods (shaded areas) are limited to either side of the equinoxes (E).
122x270mm (300 x 300 DPI)

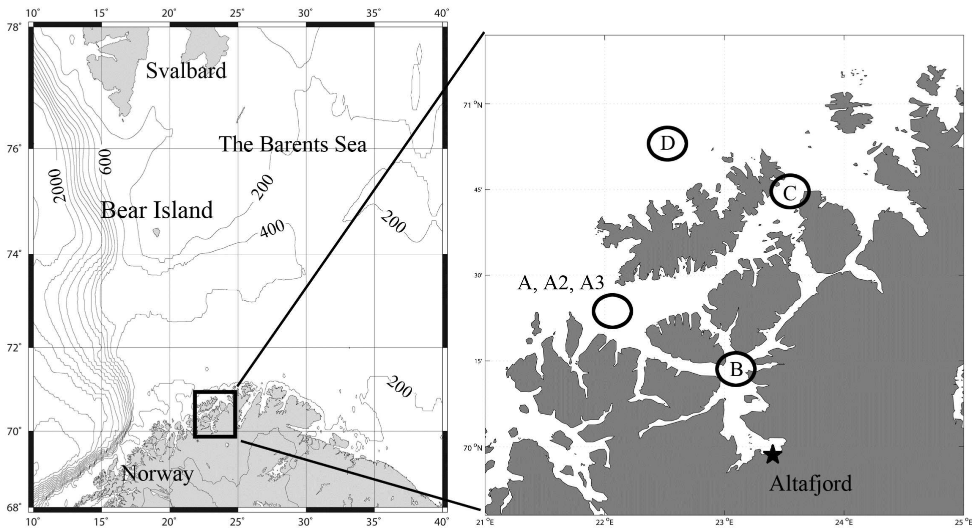

Figure 2. The study area in northern Norway. The standard model start location (A) is located near the entrance to the Altafjord. Sensitivity analyses of the model tested various other start locations, indicated as B, C, and D. The black star denotes the release location, where the Alta River enters the Altafjord.
199x123mm (300 x 300 DPI)

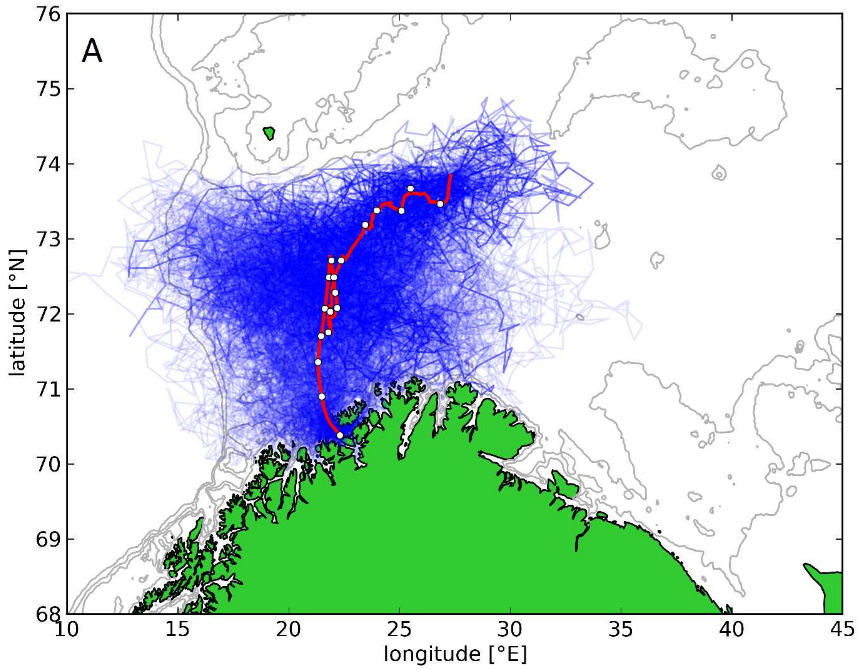

Figure 3a
677x508mm (120 x 120 DPI)

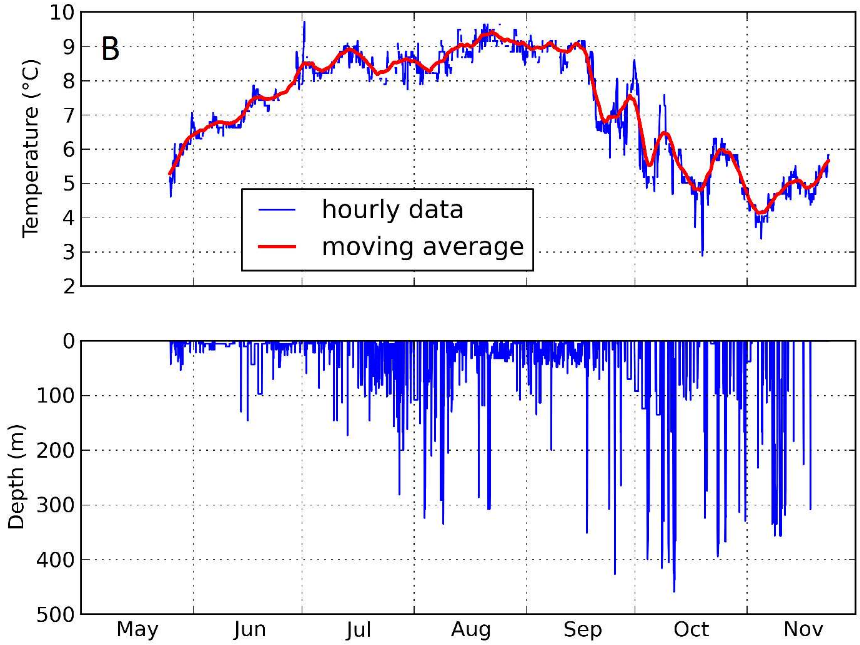

Figure 3b
677x508mm (120 x 120 DPI)

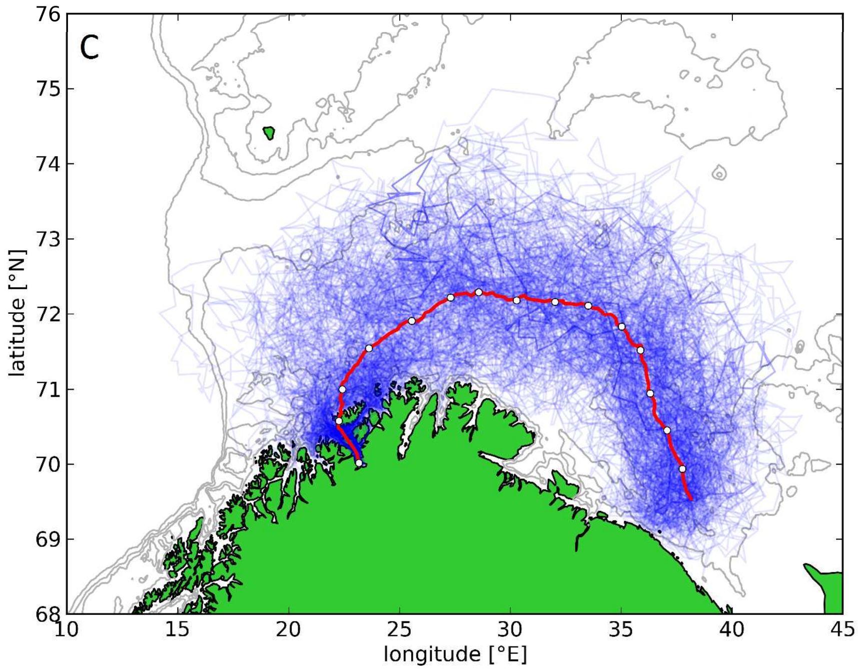

Figure 3c
677x508mm (120 x 120 DPI)

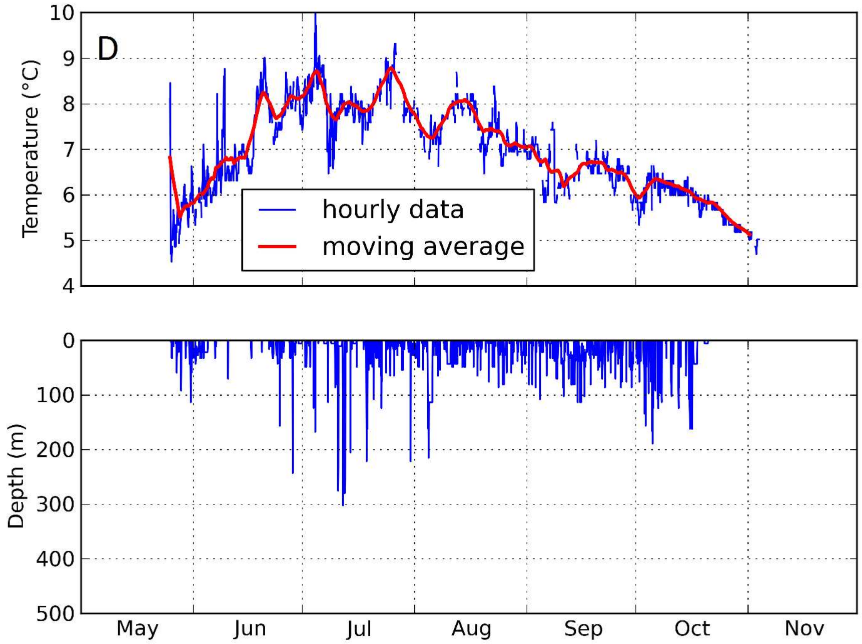

Figure 3d. A random selection of 200 possible trajectories for Tag 1 (a) and all 121 trajectories for Tag 2 (c), as well as the archived temperature and depth data from Tag 1 (b) and Tag 2 (d). The red curves in (a) and (c) give the mean of all tracks, and the white disks indicate 10-day intervals.
677x508mm (120 x 120 DPI)

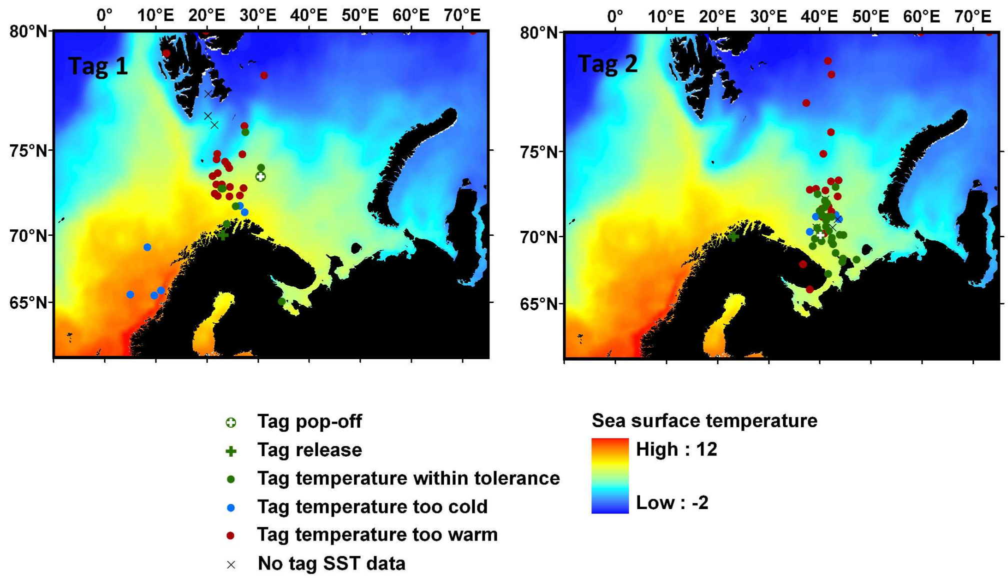

Figure 4. Map of the geolocations estimated by Tag 1 and Tag 2. Colours denote the reason for the validation or rejection of each geolocation.
918x549mm (120 x 120 DPI)

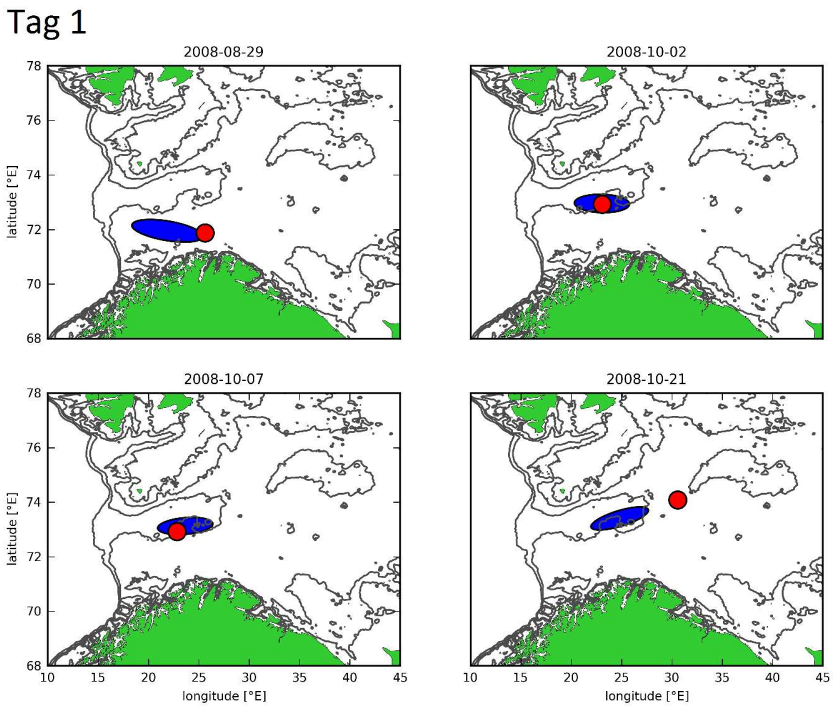

Figure 5a
677x508mm (120 x 120 DPI)

Tag 2

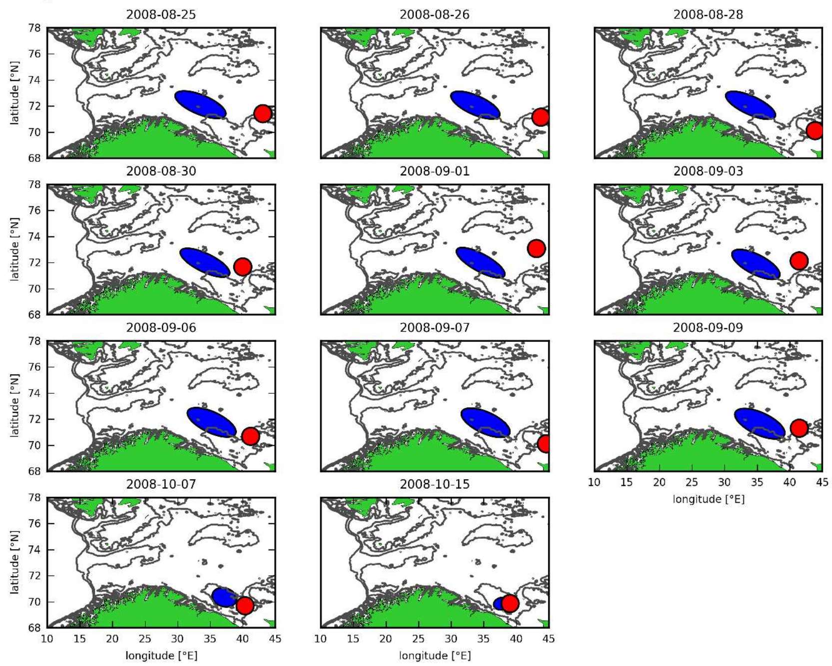

Figure 5b. Snapshot plots of the centre of gravity (± the standard deviation as an ellipse) for the trajectory particle locations (blue ovals) at the time of each geolocation (red circle) for Tag 1 and Tag 2.
677x508mm (120 x 120 DPI)

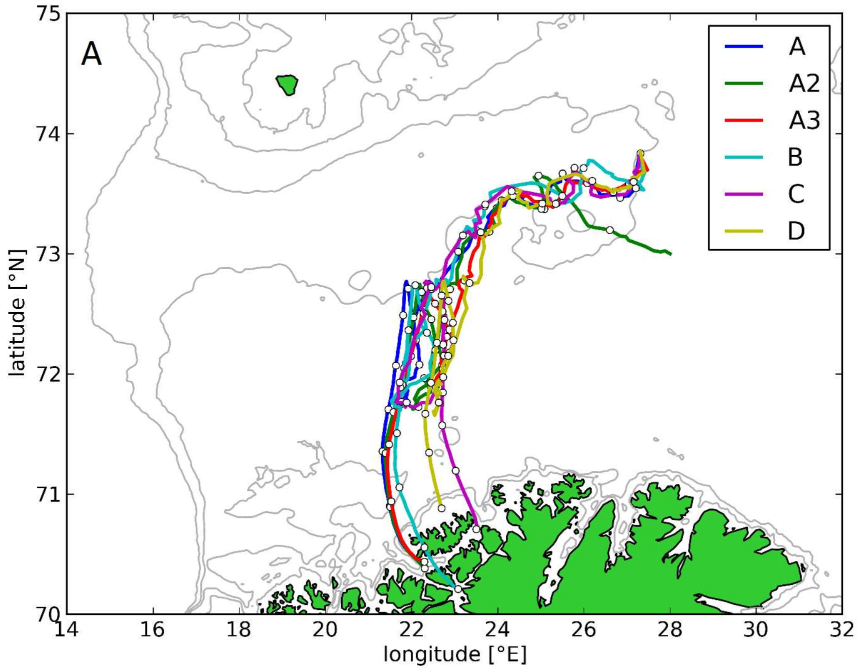

Figure 6a
677x508mm (120 x 120 DPI)

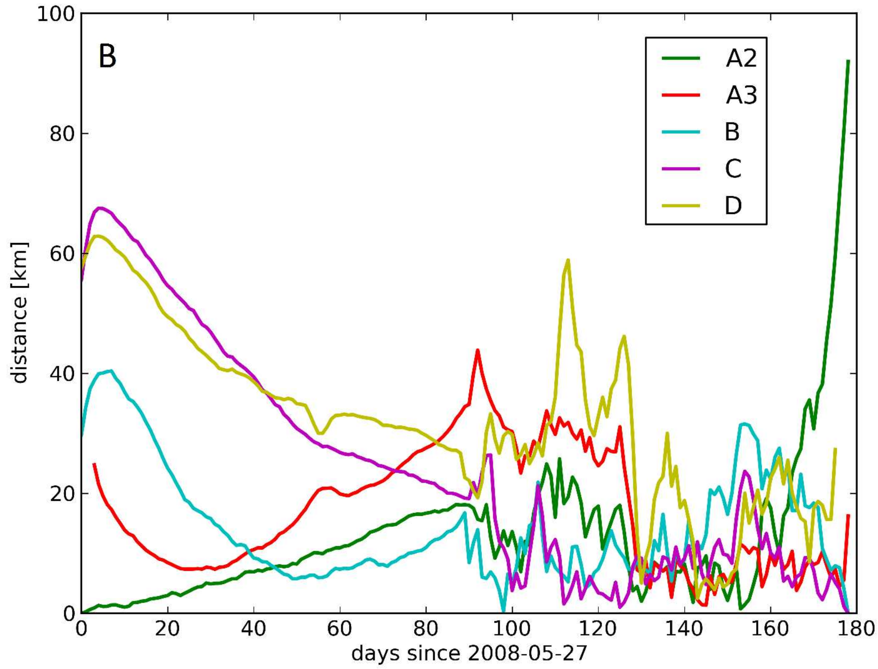

Figure 6b. Sensitivity analysis plots of the mean trajectories (a) and distances from the standard run A over time (b) for Tag 1. Parameters for each run are given in Table 2.
677x508mm (120 x 120 DPI)

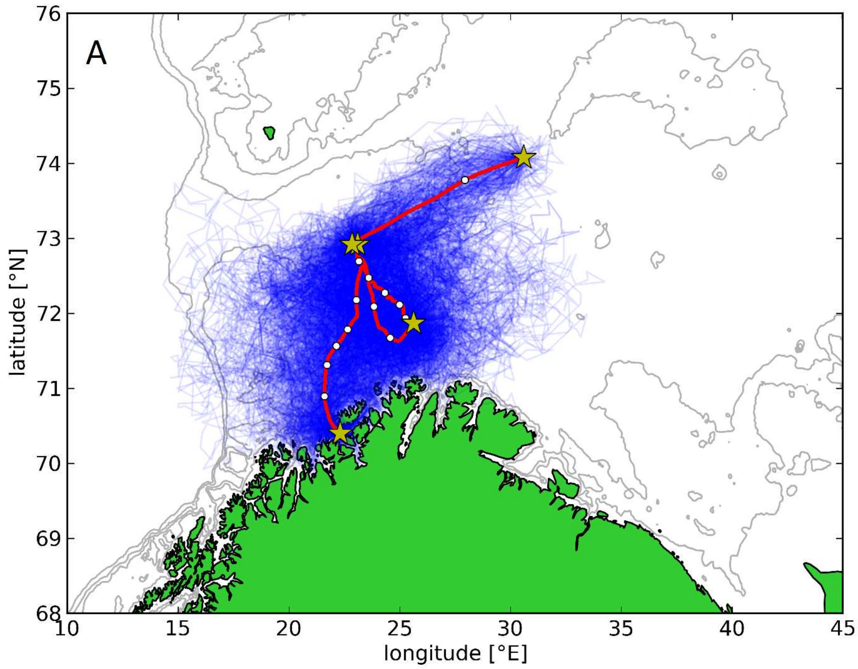

Figure 7
677x508mm (120 x 120 DPI)

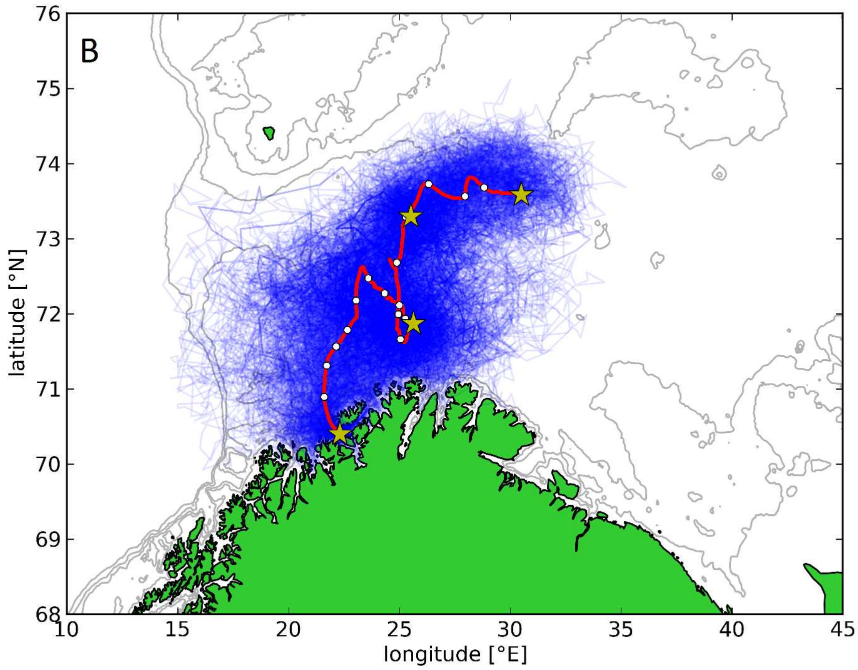

Figure 7b
677x508mm (120 x 120 DPI)

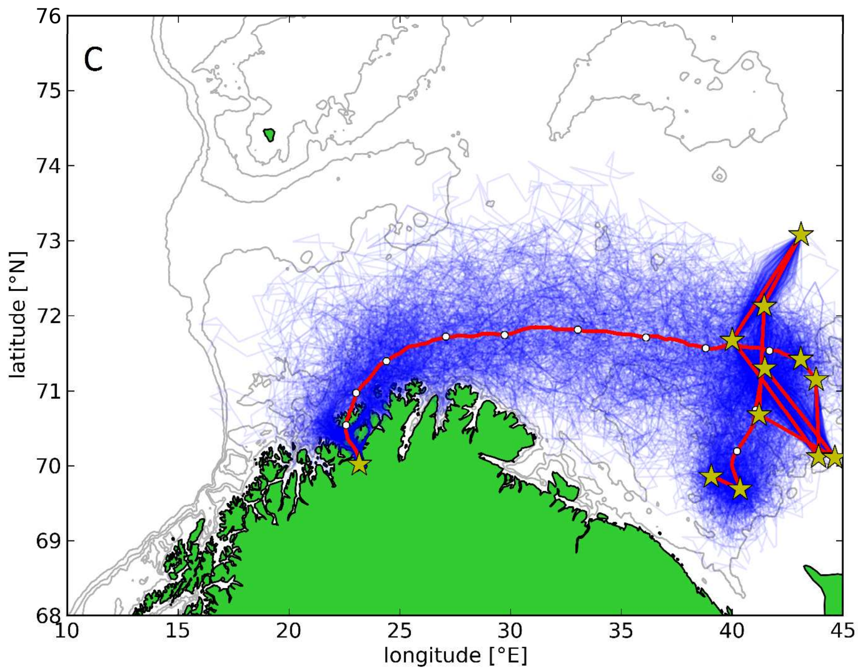

Figure 7c
677x508mm (120 x 120 DPI)

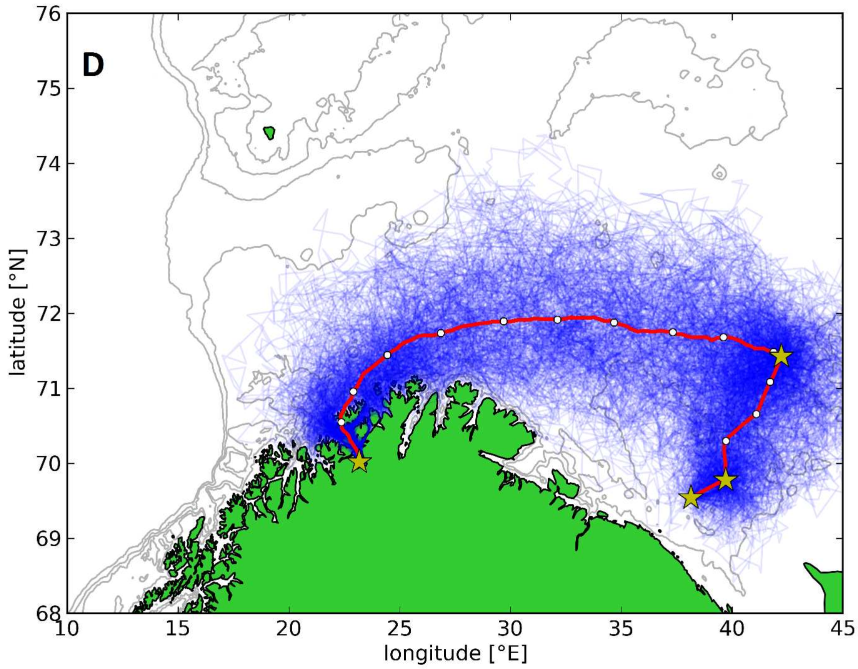

Figure 7d. Constraining the model through validated geolocations from Tag 1 (a) and Tag 2 (c). Averaging the pre-equinox and post-equinox geolocations for Tag 1 (b) and Tag 2 (d) smoothed the error found in the individual geolocation estimates to show a more general migratory pathway. The release, pop-up and geolocation positions are denoted by stars.
677x508mm (120 x 120 DPI)

Table 1. Model parameters for the standard run.

Parameter	*Symbol*	*Value*	*Units*
Max. deterministic swimming speed		0.9	m/s
Random swimming speed		2.0	m/s
Depth factor	*a*	1.2	
Additive extra depth	H_0	30	m
Temperature tolerance	dT	1.0	°C

Table 2. Sensitivity analysis parameters run on the model using Tag 1, where A is the standard run.

Run	*Start date*	*Start longitude*	*Start latitude*	*End date*	*End longitude*	*End latitude*
A	2008-05-27	22.300ºE	70.400ºN	2008-11-21	27.313ºE	73.834ºN
A2	2008-05-27	22.300ºE	70.400ºN	2008-11-21	28.000ºE	73.000ºN
A3	2008-05-30	22.300ºE	70.400ºN	2008-11-22	27.313ºE	73.834ºN
B	2008-05-25	23.080ºE	70.204ºN	2008-11-21	27.313ºE	73.834ºN
C	2008-05-27	23.500ºE	70.700ºN	2008-11-21	27.313ºE	73.834ºN
D	2008-05-27	22.700ºE	70.900ºN	2008-11-21	27.313ºE	73.834ºN